

ENERGY DISSIPATION ON EMBANKMENT DAM STEPPED SPILLWAYS, OVERFLOW STEPPED WEIRS AND MASONRY STEPPED SPILLWAYS

Prof. Hubert Chanson¹ and Stefan Felder

¹School of Civil Engineering, The University of Queensland, Brisbane QLD 4072, Australia. Tel - ++ 61 7 3365 3516, Fax - ++ 61 7 3365 4599 h.chanson@uq.edu.au

Abstract

Stepped spillways are designed to increase the rate of energy dissipation on the chute reducing the size of a downstream energy dissipator. The prediction of the turbulent dissipation above the steps constitutes a critical part of the design process, especially at large discharges per unit width corresponding to the skimming flow regime. Herein new measurements were conducted in a large facility with a channel slope of 26.6° and step heights of 0.10 m. The experiments were performed with large discharges corresponding to Reynolds numbers ranging from 5×10^4 to 1×10^6 . The waters were highly turbulent and they dissipated a major proportion of the flow kinetic energy. Taking into account the free-surface aeration, the present results were compared with recent results on 15.9° and 21.8° slopes; the range of slopes (1V:3.5H to 1V:2H) was typical of embankment slopes and older spillway designs. The comparative results yielded some simple design guidelines applicable to masonry stepped spillways, embankment dam stepped chutes and overflow stepped weirs.

Key Words : Stepped spillways, Overflow stepped weirs, Turbulent kinetic energy dissipation, Embankment structures, Masonry spillways, Air-water flows, Residual energy

1. INTRODUCTION

In recent years, the design floods of a number of reservoirs were re-evaluated and the revised outflows were often larger than those used in the original spillway designs. In many cases, the occurrence of these floods would result in dam overtopping because of the insufficient storage and spillway capacity of the existing reservoir with catastrophic consequences. Figure 1 illustrates the damage to a masonry stepped spillway that passed 2 to 3 times its design discharge capacity. This example is not unique and several similar accidents occurred very recently in UK for example (Mason and Hinks 2008, Walker 2008). A number of embankment overtopping protection systems were developed (ASCE 1994) and a common technique is the construction of a stepped spillway on the downstream slope. The stepped spillway is designed to increase the rate of energy dissipation on the chute (Chanson 2001) and the design engineer must predict accurately the turbulent dissipation above the steps, in particular for large discharges per unit width corresponding to the skimming flow regime. A characteristic feature of the skimming flow is the high level of free-surface aeration (Rajaratnam 1990, Matos 2000). Through the air-water interface, air is continuously trapped and released, and the resulting two-phase mixture interacts with the flow turbulence yielding some intricate air-water structure associated with complicated energy dissipation mechanisms (Chanson and Toombes 2002, Gonzalez and Chanson 2004, Carosi and Chanson 2008).

Although the prediction of the turbulent dissipation above the steps constitutes a critical design stage, the literature is skewed towards steep stepped slopes typical of modern gravity dams (Fig. 2A). Herein new measurements were conducted in a large facility with a channel slope of 26.6° and step heights of 0.10 m. The experiments were performed with large dimensionless discharges corresponding to Reynolds numbers ranging from 5×10^4 to 1×10^6 . Taking into account the free-surface aeration, the present results were compared with earlier results on 15.9° and 21.8° slopes. These slopes (1V:3.5H to 1V:2H) are typical of embankment slopes and older spillway designs (Fig. 2B, 2C & 2D).

CHANSON, H., and FELDER, S. (2010). "Energy Dissipation on Embankment Dam Stepped Spillways, Overflow Stepped Weirs and Masonry Stepped Spillways." *Proc. of 17th Congress of IAHR Asia and Pacific Division*, IAHR-APD, Auckland, New Zealand, 21-24 Feb., B. MELVILLE, G. DE COSTA, and T. SWANN Eds., 10 pages (ISBN 0-86869-125-9).



Fig. 1 - Damaged stepped spillway at Boltby dam (UK) (Courtesy of Peter MASON) - Damage during 19 June 2005 flood, peak flow: 22-30m³/s



(A) Elkwater Fork dam stepped spillway construction in 2007 (Courtesy of Craig Savelle, USDA-NRCS-NDCSMC) - H = 29 m, h = 0.61 m, W = 46 m, RCC construction completed in 2008

(B) Opuha dam stepped spillway in operation (Courtesy of Tonkin & Taylor) - H = 50 m, 26.6° slope



(C) Gold Creek dam stepped spillway on 12 January 2009 (Courtesy of Gordon Griggs) - H = 26 m, h = 1.5 m, 20.6° slope, W = 55 m, concrete stepped spillway completed in 1890

(D) Stepped spillway of Salado Creek Dam Site 15R (Courtesy of Craig Savelle, USDA-NRCS-NDCSMC) - h = 0.61 m, 21.8° slope, RCC construction

Fig. 2 - Photographs of stepped spillways

CHANSON, H., and FELDER, S. (2010). "Energy Dissipation on Embankment Dam Stepped Spillways, Overflow Stepped Weirs and Masonry Stepped Spillways." *Proc. of 17th Congress of IAHR Asia and Pacific Division*, IAHR-APD, Auckland, New Zealand, 21-24 Feb., B. MELVILLE, G. DE COSTA, and T. SWANN Eds., 10 pages (ISBN 0-86869-125-9).

2. EXPERIMENTAL FACILITIES

New experiments were conducted at the University of Queensland in a 3.2 m long, 1 m wide chute (26.6° slope) with flow rates ranging from 14 to 250 L/s. The chute consists of a broad-crest followed by 10 identical steps ($h = 0.10$, $l = 0.20$ m). The open channel facility is a permanent facility and the inflow quality has been verified in this and previous studies (Jempson 2001, Gonzalez and Chanson 2007). The waters are supplied by a pump controlled with adjustable frequency AC motor drive enabling an accurate discharge adjustment. The water discharge was measured from the upstream head above the crest, and the head-discharge relationship was checked with detailed velocity measurements on the crest itself (Gonzalez and Chanson 2007). The clear-water flow depths were measured with a point gauge. The air-water flow properties were recorded using a double-tip resistivity probe ($\varnothing = 0.25$ mm, Pt). The two tips were aligned in the direction of the flow and the longitudinal separation was 7.5 mm. The phase detection probe was excited by an electronic system (Ref. UQ82.518) designed with a response time less than 10 μ s and calibrated with a square wave generator. The probe signals were sampled at 20 kHz per sensor for 45 s. The analysis of the phase-detection probe signal provided some point measurements in terms of the void fraction C and bubble count rate F defined as the number of bubbles, or droplets, impacting a probe sensor per second. The double-tip conductivity probe provided also the local mean air-water interface velocity V and chord length distributions. Note that V was a time-averaged measurement spatially-averaged between the probe sensors.

The translation of the probe in the direction normal to the pseudo-bottom formed by the step edges was controlled by a fine adjustment traverse mechanism connected to a Mitutoyo™ digimatic scale unit with an accuracy of less than 0.2 mm.

Slope θ (°)	Step height h (m)	Reynolds number Re	Geometry	Reference(s)
Laboratory studies				
26.6	0.10	5E+4 to 1E+6	Horizontal steps	Present study
26.6	0.025 0.05	4E+4 to 6E+4	Horizontal steps	Meireles et al. (2006)
21.8	0.05 0.10	3E+4 to 8E+5 3E+4 to 7E+5	Horizontal steps	Felder & Chanson (2009) Carosi & Chanson (2008)
15.9	0.05 0.10	8E+4 to 8E+5 3E+5 to 8E+5	Horizontal steps	Gonzalez & Chanson (2004) Chanson & Toombes (2002)
5.7, 11.3, 18.8	0.025 to 0.05	9E+4 to 3E+5	Horizontal steps	Yasuda & Ohtsu (1999)
Prototype studies				
18.4	0.19	9.5E+5 to 1.2E+6	Brushes Clough dam spillway, inclined downward steps	Baker (1994)
8.75	0.405	7E+6 to 2E+8	Dneiper powerplant, horizontal steps	Grinchuk et al. (1977)

Table 1 - Experimental investigation of stepped spillways on moderate slopes

2.1 Experimental flows

On a stepped chute, the waters flow as a succession of free-falling nappes (i.e. nappe flow) at low flow rates. At large flow rates with an identical chute geometry (step height, mean slope), the water skims over the pseudo-invert formed by the step edges (i.e. skimming flow). For some intermediate discharges, a transition flow regime is observed, characterised by a chaotic behaviour and strong splashing and droplet projections downstream of the inception point of free-surface aeration.

The present observations indicated a nappe flow regime for dimensionless discharges $d_c/h < 0.5$ and a skimming flow regime for $d_c/h > 0.9$, where d_c is the critical flow depth ($d_c = \sqrt[3]{Q^2 / (g \times W^2)}$) and h is the vertical step height. The results were in agreement the literature (Chanson 2001).

The air-water flow measurements were conducted with dimensionless discharges d_c/h between 1.01 and 1.85. The probe sensors were located on the channel centreline at the step edges for all flow rates.

CHANSON, H., and FELDER, S. (2010). "Energy Dissipation on Embankment Dam Stepped Spillways, Overflow Stepped Weirs and Masonry Stepped Spillways." *Proc. of 17th Congress of IAHR Asia and Pacific Division*, IAHR-APD, Auckland, New Zealand, 21-24 Feb., B. MELVILLE, G. DE COSTA, and T. SWANN Eds., 10 pages (ISBN 0-86869-125-9).

The flow conditions corresponded to Reynolds numbers ranging from 4×10^5 to 1.0×10^6 where $Re = \rho \times U_w \times D_H / \mu$ with ρ and μ the water density and viscosity respectively, U_w the flow velocity and D_H the hydraulic diameter. The details are summarised in Table 1 and compared with earlier studies conducted on slopes between 8.75 and 26.6° with large Reynolds numbers to minimise the potential scale effects. These were specifically discussed by Chanson (2008) and Felder and Chanson (2009).



(A) $d_c/h = 1.15$, inception of free-surface aeration at step edge 4

(B) $d_c/h = 1.36$, inception of free-surface aeration between step edges 5 and 6



(C) $d_c/h = 1.59$, inception of free-surface aeration at step edge 6

(D) $d_c/h = 1.85$, inception of free-surface aeration at step edge 8

Fig. 3 - Experimental flow patterns

3. EXPERIMENTAL OBSERVATIONS

3.1 Presentation

On the stepped channel, the waters were non-aerated at the upstream end of the chute. Some free-surface aeration occurred when the turbulent shear next to the free-surface exceeded the bubble resistance offered by surface tension and buoyancy. Downstream of the inception point of free-surface aeration, some strong air-water mixing took place (Fig. 3). Large amounts of air were entrained, and very-strong interactions between main stream turbulence, step cavity recirculation zones and free-surface were observed associated with dissipative processes.

The location L_I of the inception point of free-surface aeration was recorded. Herein L_I is the longitudinal distance measured from the downstream end of the broad-crest (step edge 1). Typical results are presented in a dimensionless form in Figure 4 where the experimental data are compared with the empirical correlation:

$$(1) \quad \frac{L_I}{h \times \cos \theta} = 9.719 \times (\sin \theta)^{0.0796} \times \left(\frac{q}{\sqrt{g \times \sin \theta \times (h \times \cos \theta)^3}} \right)^{0.713}$$

where θ is the angle between the slope formed by the step edges and the horizontal, q is the water discharge per unit width ($q = Q/W$) and g is the gravity acceleration. Equation (1) was developed for

steep stepped chutes and was validated with both prototype and laboratory data (Chanson 1995,2001). It is plotted in Figure 4 for $\theta = 21.8^\circ$ and compared with several experimental data sets. All the data showed that the location of the air entrainment L_1 shifted downstream with increasing flow rate. At the limit, the skimming flow became non-aerated when L_1 was larger than the length of the stepped channel.

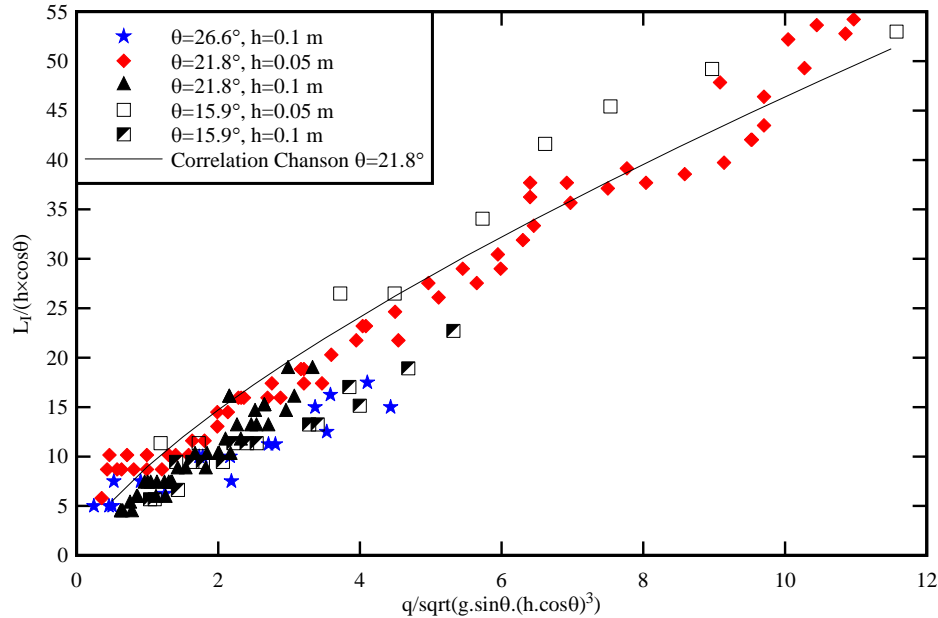


Fig. 4 - Dimensionless location $L_1/(h \times \cos\theta)$ of the inception point of free-surface aeration on stepped spillways with $15.9^\circ \leq \theta \leq 26.6^\circ$ - Comparison with Equation (1) calculated for $\theta = 21.8^\circ$

3.2 Air-water flow properties

The experiments highlighted some substantial free-surface aeration at and immediately downstream of the inception point of free-surface aeration, while the flow aeration remained sustained further downstream all along the chute (Fig. 3). Figure 5 illustrates some typical dimensionless distributions of void fraction, bubble count rate and velocity downstream of the inception point for two flow rates. In skimming flows, the void fraction distributions presented a smooth shape that followed closely the analytical solutions of the advective diffusion for air bubbles:

$$(2) \quad C = 1 - \tanh^2 \left(K' - \frac{y'}{2 \times D_o} + \frac{\left(y' - \frac{1}{3} \right)^3}{3 \times D_o} \right) \quad \text{at step edge}$$

where C is the void fraction, $y' = y/Y_{90}$, y is distance measured normal to the pseudo-invert formed by the step edges, Y_{90} is the characteristic distance where $C = 90\%$. K' is an integration constant and D_o is a function of the depth-averaged void fraction C_{mean} only:

$$(3) \quad K' = 0.32745 + 1/(2 \times D_o) - 8/(81 \times D_o)$$

$$(4) \quad C_{\text{mean}} = 0.762 \times (1.0434 - \exp(-3.614 \times D_o))$$

where the depth-averaged void fraction C_{mean} is defined as:

$$(5) \quad C_{\text{mean}} = \int_0^1 (1-C) \times dy'$$

Equation (2) was first developed by Chanson and Toombes (2002) and it is compared with experimental data in Figure 5.

The dimensionless distributions of bubble count rate showed consistently a characteristic shape with a maximum value F_{max} observed for void fractions between 0.40 and 0.55. This is seen in Figure 5 with the dimensionless bubble count rate data F/F_{max} . A characteristic feature of all the experiments (not

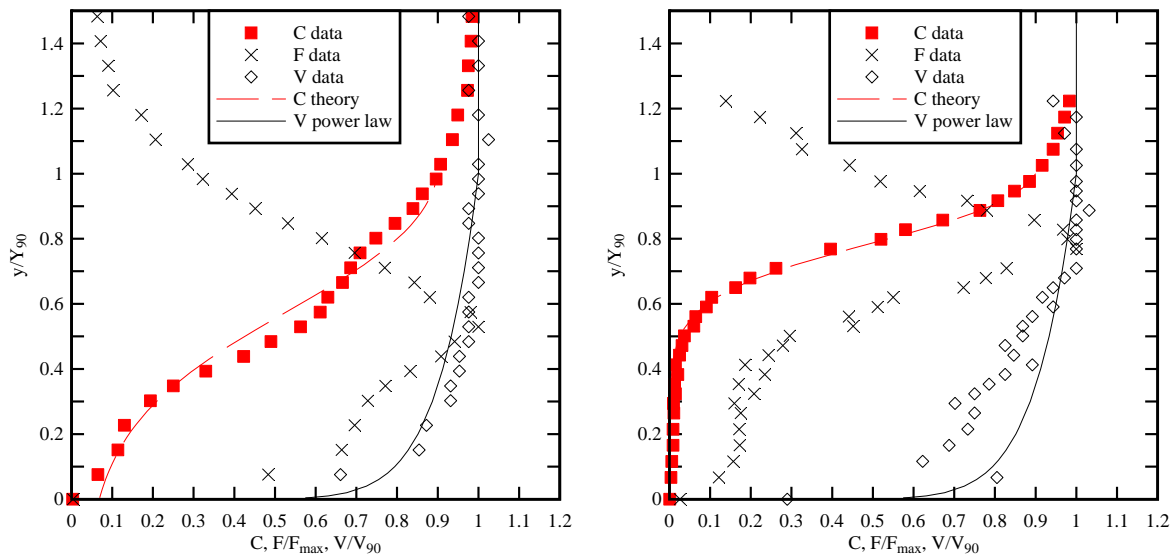
shown in Fig. 5) was a distinct seesaw pattern in terms of the dimensionless maximum bubble count rate $F_{\max} \times d_c / V_c$ and depth-averaged void fraction C_{mean} . This oscillating pattern had a wave length of about two step cavities. Such a pattern was observed before for a range of slopes and step heights (Boes 2000, Chanson and Toombes 2002, Yasuda and Chanson 2003, Felder and Chanson 2009). It is believed to result from the strong interferences between vortex shedding in the shear layers behind each step edge and the free-surface. Another feature was that the two-phase flow properties did not reach uniform equilibrium before the end of the chute. This was observed herein for all discharges in the present study.

The dimensionless distributions of interfacial velocity showed a characteristic shape. At each step edge, the velocity distributions compared favourably with a power-law function for $y' = y/Y_{90} < 1$ and with an uniform profile for $y/Y_{90} > 1$:

$$(6) \quad \frac{V}{V_{90}} = y'^{1/N}$$

$$(7) \quad \frac{V}{V_{90}} = 1$$

where V_{90} is the characteristic air-water velocity at $y = Y_{90}$. Several studies yielded Equation (6) (e.g. Matos 2000, Boes 2000, Chanson and Toombes 2002, Gonzalez and Chanson 2004), but a few documented the velocity distribution in the upper spray region (Carosi and Chanson 2008, Felder and Chanson 2009). Equations (6) and (7) are compared with the experimental data in Figure 5. In the present study, the velocity power law exponent was about 1/10 in average (i.e. $N = 10$), although it varied between adjacent step edges. Such fluctuations were believed to be caused by some complicated interference between adjacent shear layers and cavity flows.



(A) $d_c/h = 1.0$, $Re = 4 \times 10^5$, step edge 10, $Y_{90} = 0.066$ m, $V_{90} = 3.66$ m/s, $F_{\max} = 255$ Hz, $C_{\text{mean}} = 0.46$

(B) $d_c/h = 1.85$, $Re = 1 \times 10^6$, step edge 10, $Y_{90} = 0.101$ m, $V_{90} = 4.54$ m/s, $F_{\max} = 76.4$ Hz, $C_{\text{mean}} = 0.21$

Fig. 5 - Dimensionless distributions of void fraction C , bubble count rate F/F_{\max} and velocity V/V_{90} in air-water skimming flows on a stepped spillway

3.3 Energy dissipation and flow resistance in skimming flows

The rate of energy dissipation $\Delta H/H_{\max}$ and the dimensional residual energy H_{res}/d_c were estimated at several steps along the chute based upon the detailed air-water flow measurements. Herein H_{\max} is the upstream total head above the step location, $\Delta H = H_{\max} - H_{\text{res}}$, and the residual head H_{res} is the specific energy of the flow at the sampling location:

$$(8) \quad H_{\text{res}} = d \times \cos \theta + \frac{U_w^2}{2g}$$

where U_w is the flow velocity ($U_w = q/d$) and d is the equivalent clear-water depth defined as:

$$(9) \quad d = \int_{y'=0}^1 (1 - C) \times dy'$$

The present results showed a decreasing rate of energy dissipation on the stepped chute with increasing discharge from about $\Delta H/H_{\max} = 60\%$ for $d_c/h < 1.2$ down to 50% for $d_c/h = 1.85$. The trend was consistent with earlier studies (Matos 2000, Chanson 1995).

For the design engineer, the dimensionless residual head H_{res}/d_c is a key design parameter because it quantifies the kinetic energy to be dissipated in a downstream stilling structure. The residual energy data are shown in Figure 6 together with comparable experimental results. The comparative data sets regroup some results derived from detailed air-water flow measurements on three chute slopes ($\theta = 15.9^\circ, 21.8^\circ$ & 26.6°) and for a range of step heights. The comparison implied that the dimensionless residual head was about $2.3 \leq H_{\text{res}}/d_c \leq 3.7$ with an average value of 3.1 for $\theta = 21.8^\circ$, while it had a larger mean value of 4.6 for $\theta = 15.9^\circ$ and 26.6° independently of the step height (Fig. 6). The corresponding trend lines are shown with two dashed lines in Figure 6. For the smaller slope ($\theta = 15.9^\circ$), there appeared to be some dependency of the residual energy with the dimensionless discharge d_c/h ; but, for larger bed slopes, the data tended to be independent of the flow rate. The present results were obtained with a fully-developed, aerated flow at the stepped chute downstream end. For larger discharges, the flow might not be fully-developed before the downstream end, and the residual energy could be considerably larger.

The skimming flows were characterised by significant form losses. Downstream of the inception point of free-surface aeration, the average shear stress between the skimming flow and the cavity recirculation was deduced from the measured friction slope S_f . It may be expressed in terms of a dimensionless friction coefficient:

$$(10) \quad f_e = \frac{8 \times g \times S_f \times \left(\int_{y=0}^{Y_{90}} (1 - C) \times dy \right)}{U_w^2}$$

where f_e is the equivalent Darcy-Weisbach friction factor of the air-water flow, and the friction slope $S_f = -\partial H/\partial x$ is the slope of the total head line (Henderson 1966). Equation (10) gives an estimate of the Darcy-Weisbach friction factor in the air-water flow region and the data are presented in Figure 7. In Figure 7, the friction factor is plotted as a function of the dimensionless step roughness height $h \times \cos\theta/D_H$, where D_H is the hydraulic diameter. In average, the equivalent Darcy friction factor was $\overline{f_e} \approx 0.22$ downstream of the inception point of free-surface aeration for the present study. The results are compared with several data sets in Figure 7 including two prototype data sets (Table 1). All the laboratory data were close although the discrepancy with the Brushes Clough prototype data remains unexplained (Fig. 7).

The flow resistance data were compared also with a simplified analytical model of the pseudo-boundary shear stress in the developing shear layer downstream of each step edge that may be expressed in dimensionless form as: $f = 2/(K \times \sqrt{\pi})$ where $1/K$ is the dimensionless expansion rate of the shear layer (Chanson 2001). The theoretical expression predicts $f \approx 0.2$ for $K = 6$ that is close to the observations (Fig. 7).

Note that both the energy dissipation and flow resistance data suggested a larger dissipation rate for $\theta = 21.8^\circ$ than for $\theta = 15.9^\circ$ and 26.6° (Fig. 6 and 7). This trend was consistent with the findings of Ohtsu et al. (2004) and Gonzalez and Chanson (2006), and the result might be linked with some wake interference mechanism between adjacent steps proposed by Chanson (1995)

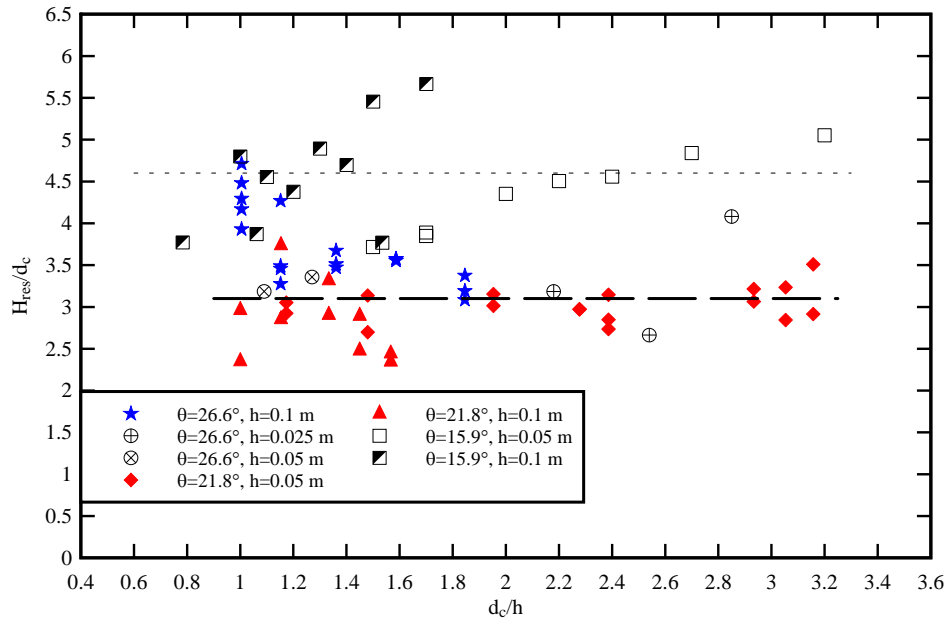


Fig. 6 - Dimensionless residual energy H_{res}/d_c in air-water skimming flows on stepped spillways with $8.75^\circ \leq \theta \leq 26.6^\circ$

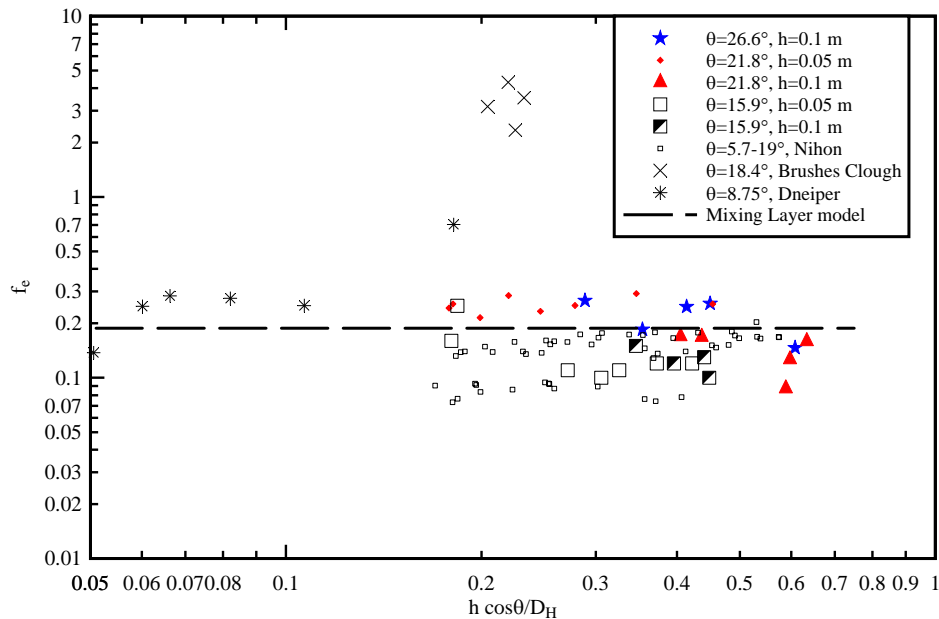


Fig. 7 - Friction factor f_c in air-water skimming flows on stepped spillways with $8.75^\circ \leq \theta \leq 26.6^\circ$

4. DISCUSSION

In skimming flows, the basic mechanisms of turbulent dissipation included cavity recirculation, momentum exchange with the free stream, and interactions between free-surface and mainstream turbulence. The interactions between mixing layer and horizontal step face, and skin friction at the step downstream end contributed to further energy dissipation on moderate slopes similar to the present configurations. At each step edge, highly coherent small-scale vortices were formed abruptly at the step corner because of the large gradient of vorticity at the corner. The initial region of the mixing layer was dominated by a train of sequential small-scale vortices which eventually paired to form large scale vortical structures that are advected downstream. The three dimensional nature of recirculating vortices is believed to play a role to further the rate of energy dissipation. Gonzalez and Chanson (2008) demonstrated quantitatively some means to enhance the flow resistance with turbulence

CHANSON, H., and FELDER, S. (2010). "Energy Dissipation on Embankment Dam Stepped Spillways, Overflow Stepped Weirs and Masonry Stepped Spillways." *Proc. of 17th Congress of IAHR Asia and Pacific Division*, IAHR-APD, Auckland, New Zealand, 21-24 Feb., B. MELVILLE, G. DE COSTA, and T. SWANN Eds., 10 pages (ISBN 0-86869-125-9).

manipulation of the cavity recirculation. More recently Carosi and Chanson (2008) showed some turbulent energy dissipation in the bulk of the aerated flow in the form of large-scale vortices. The turbulent structures were produced in the step cavities, ejected into the main flow and interacted with the "free-surface". The dissipation process was linked with both the entrapment and advection of air bubbles within the main flow and the formation and ejection of water droplets above the "free-surface".

The present findings provide some simple preliminary design guidelines that may apply to a stepped spillway system for an embankment structure and a masonry spillway with a moderate slope (1V:3.5H to 1V:2H). For a small to medium size dam, the residual head at the spillway toe may be obtained from Figure 6: $H_{res} \approx 3.1 \times d_c$ for a 1V:2.5H slope ($\theta = 21.8^\circ$), or $H_{res} \approx 4.6 \times d_c$ for larger or smaller slopes between 1V:3.5H and 1V:2H. The application of the continuity equation and the definition of the residual head yield the supercritical flow depth and velocity at the spillway toe and entering into the stilling basin.

For a long spillway chute, the flow may become uniform equilibrium, and the continuity and momentum principles give an expression of the downstream flow velocity:

$$(11) \quad U_w = \sqrt{\frac{8 \times g}{f_e}} \times \sqrt{\frac{D_H}{4}} \times \sin \theta$$

where the Darcy-Weisbach friction factor f_e for the air-water skimming flow is deduced from Figure 7: $f_e \approx 0.2$ to 0.25 .

The proposed method may be used for the preliminary design calculations and the final design must be validated with some physical modelling in a relatively large-size model.

5. CONCLUSION

In this study, the energy dissipation performances of stepped spillways were investigated experimentally in a large size physical model. The focus was the characteristics of the air-water skimming flows on slopes between 1V:3.5H to 1V:2H ($\theta = 15.9^\circ$ to 26.6°) that are typical of old masonry spillways, embankments and overflow weirs. The experiments conducted with Reynolds numbers between 5×10^4 and 1×10^6 demonstrated the considerable free-surface aeration as well as the significant energy dissipation rate on the steps. On small weirs and dams, a key design parameters is the dimensionless residual head at the downstream end of the chute H_{res}/d_c and Figure 6 provides some design guidelines for slopes between 1V:3.5H to 1V:2H. For higher dams where the flow may become uniform equilibrium before the downstream end of the stepped chute, the application of the momentum principle (Eq. (11)) together with Figure 7 enables an accurate prediction of the flow properties at the chute downstream end.

Interestingly the experimental results confirmed earlier findings that the rate of energy dissipation tends to be maximum for a slope of 1V:2.5H ($\theta = 21.8^\circ$). It is suggested that some wake interference mechanism between adjacent steps may be trigger a greater rate of energy dissipation associated with a larger flow resistance. For shallower or steeper slopes, the energy dissipation rate is slightly lower, although it is still one to two orders of magnitude larger than on a smooth invert spillway.

ACKNOWLEDGEMENTS

The authors acknowledge the technical assistance of Ahmed Ibrahim, Graham Illidge and Clive Booth. The experimental measurements were undertaken by Henry Cheung and Rhys Collins.

REFERENCES

- ASCE Task Committee (1994). "Alternatives for Overtopping Protection of Dams." *ASCE*, New York, USA, Task Committee on Overtopping Protection, 139 pages.
- Baker, R. (1994). "Brushes Clough Wedge Block Spillway - Progress Report No. 3." *SCEL Project Report No. SJ542-4*, University of Salford, UK, Nov., 47 pages.
- Boes, R.M. (2000). "Zweiphasenstroömung und Energieumsetzung an Grosskaskaden." ("Two-Phase Flow and Energy Dissipation on Cascades.") *Ph.D. thesis*, VAW-ETH, Zürich, Switzerland (in German). (also *Mitteilungen der Versuchsanstalt für Wasserbau, Hydrologie und Glaziologie*, ETH-Zürich, Switzerland, No. 166).

- CHANSON, H., and FELDER, S. (2010). "Energy Dissipation on Embankment Dam Stepped Spillways, Overflow Stepped Weirs and Masonry Stepped Spillways." *Proc. of 17th Congress of IAHR Asia and Pacific Division*, IAHR-APD, Auckland, New Zealand, 21-24 Feb., B. MELVILLE, G. DE COSTA, and T. SWANN Eds., 10 pages (ISBN 0-86869-125-9).
- Carosi, G., and Chanson, H. (2008). "Turbulence Characteristics in Skimming Flows on Stepped Spillways." *Canadian Journal of Civil Engineering*, Vol. 35, No. 9, pp. 865-880 (DOI:10.1139/L08-030).
- Chanson, H. (1995). "Hydraulic Design of Stepped Cascades, Channels, Weirs and Spillways." *Pergamon*, Oxford, UK, Jan., 292 pages.
- Chanson, H. (2001). "The Hydraulics of Stepped Chutes and Spillways." *Balkema*, Lisse, The Netherlands, 418 pages.
- Chanson, H. (2008). "Physical Modelling, Scale Effects and Self-Similarity of Stepped Spillway Flows." *Proc. World Environmental and Water Resources Congress 2008 Ahupua'a*, ASCE-EWRI, 13-16 May, Hawaii, R.W. Badcock Jr and R. Walton Eds., Paper 658, 10 pages (CD-ROM).
- Chanson, H., and Toombes, L. (2002). "Experimental Investigations of Air Entrainment in Transition and Skimming Flows down a Stepped Chute." *Canadian Journal of Civil Engineering*, Vol. 29, No. 1, pp. 145-156.
- Felder, S., and Chanson, H. (2009). "Turbulence, Dynamic Similarity and Scale Effects in High-Velocity Free-Surface Flows above a Stepped Chute." *Experiments in Fluids*, Vol. 47, No. 1, pp. 1-18 (DOI: 10.1007/s00348-009-0628-3).
- Gonzalez, C.A., and Chanson, H. (2004). "Interactions between Cavity Flow and Main Stream Skimming Flows: an Experimental Study." *Canadian Journal of Civil Engineering*, Vol. 31, No. 1, pp. 33-44.
- Gonzalez, C.A., and Chanson, H. (2006). "Flow Characteristics of Skimming Flows in Stepped Channels. Discussion." *Journal of Hydraulic Engineering*, ASCE, Vol. 132, No. 5, pp. 537-539 (DOI: 10.1061/(ASCE)0733-9429(2006)132:5(537))
- Gonzalez, C.A., and Chanson, H. (2007). "Experimental Measurements of Velocity and Pressure Distribution on a Large Broad-Crested Weir." *Flow Measurement and Instrumentation*, Vol. 18, No. 3-4, pp. 107-113 (DOI 10.1016/j.flowmeasinst.2007.05.005).
- Gonzalez, C.A., and Chanson, H. (2008). "Turbulence and Cavity Recirculation in Air-Water Skimming Flows on a Stepped Spillway." *Journal of Hydraulic Research*, IAHR, Vol. 46, No. 1, pp. 65-72.
- Grinchuk, A.S., Pravdivets, Y.P., and Shekhtmann, N.V. (1977). "Test of Earth Slope Revetments Permitting Flow of Water at Large Specific Discharges." *Gidrotekhnicheskoe Stroitel'stvo*, No. 4, pp. 22-26 (in Russian). (Translated in *Hydrotechnical Construction*, 1978, Plenum Publ., pp. 367-373).
- Henderson, F.M. (1966). "Open Channel Flow." *MacMillan Company*, New York, USA.
- Jempson, M.A. (2001). "Flood and Debris Loads on Bridges." *Ph.D. thesis*, Univ. of Queensland, Dept. of Civil Eng., Australia, May, 429 pages.
- Mason, P.J., and Hinks, J.L. (2008). "Security of Stepped Masonry Spillways: Lessons from Ulley Dam." *Dams and Reservoirs*, Vol. 18, No. 1, pp. 5-8.
- Matos, J. (2000). "Hydraulic Design of Stepped Spillways over RCC Dams." *Intl Workshop on Hydraulics of Stepped Spillways*, Zürich, Switzerland, H.E. Minor & W.H. Hager Editors, Balkema Publ., pp. 187-194.
- Meireles, I., Cabrita, J., and Matos, J. (2006). "Non-Aerated Skimming Flow Properties on Stepped Chutes over Small Embankment Dams." *Proc. International Junior Researcher and Engineer Workshop on Hydraulic Structures*, IAHR, Montemor-o-Novo, Portugal, 2-4 Sept., J. Matos and H. Chanson Ed., Hydraulic Model Report No. CH61/06, Div. of Civil Engineering, The University of Queensland, Brisbane, Australia, pp. 91-99.
- Ohtsu, I., Yasuda, Y., and Takahashi, M. (2004). "Flow Characteristics of Skimming Flows in Stepped Channels." *Journal of Hydraulic Engineering*, ASCE, Vol. 130, No. 9, pp. 860-869.
- Rajaratnam, N. (1990). "Skimming Flow in Stepped Spillways." *Jl of Hyd. Engrg.*, ASCE, Vol. 116, No. 4, pp. 587-591.
- Walker, J.P. (2008). "The Discontinuance of Boltby Reservoir, North Yorkshire, UK." *Dams and Reservoirs*, Vol. 18, No. 1, pp. 17-21.
- Yasuda, Y., and Chanson, H. (2003). "Micro- and Macro-scopic Study of Two-Phase Flow on a Stepped Chute." *Proc. 30th IAHR Biennial Congress*, Thessaloniki, Greece, J. Ganoulis and P. Prinos Ed., Vol. D, pp. 695-702
- Yasuda, Y., and Ohtsu, I.O. (1999). "Flow Resistance of Skimming Flow in Stepped Channels." *Proc. 28th IAHR Congress*, Graz, Austria, Session B14, 6 pages.